

We are IntechOpen, the world's leading publisher of Open Access books Built by scientists, for scientists

6,900

Open access books available

186,000

International authors and editors

200M

Downloads

Our authors are among the

154

Countries delivered to

TOP 1%

most cited scientists

12.2%

Contributors from top 500 universities



WEB OF SCIENCE™

Selection of our books indexed in the Book Citation Index
in Web of Science™ Core Collection (BKCI)

Interested in publishing with us?
Contact book.department@intechopen.com

Numbers displayed above are based on latest data collected.
For more information visit www.intechopen.com



Application of Spin-Orbit Coupling in Exotic Graphene Structures and Biology

Richard Pinčák and Erik Bartoš

Abstract

An important measurable quantity in the carbon nanostructures, including the nanotubular part of the graphitic wormhole, is the spin-orbit coupling. We will present in this chapter spin-orbit coupling for the fermions located in exotic graphene structures as is graphene wormhole and also in biological systems. Considering this influence, the two-component Dirac equation is changed into the usual four-component form. As a consequence, the chiral fermions should be detected close to the wormhole bridge. We will show that the smaller is the radius of the wormhole bridge, the stronger this effect should be. Finally, we will describe the role of spinor fields in the time series of genetic code. The reversed transcription process of the gene expression could be defined by a moduli state space model of a coupling spinor field between the gene of a viral particle and the host cell. As a general result, all states of codon can be computed by the Chern-Simons 3-forms.

Keywords: spinor network structure, spin orbit coupling, Chern-Simons fields, graphene wormhole, genetic code

1. Graphitic wormhole

The investigation of unique chemical and mechanical properties of nanostructures, e.g., fullerene, graphene, and nanotubes, promises a wide application in many technical areas. The electronic properties of the nanostructures are basically defined by their hexagonal carbon lattice structure and its variations. New promising results are expected with the preparation of more complicated forms as a wormhole. The wormhole is usually composed of two different kinds of nanostructure: two graphene sheets are connected together with the help of a connecting nanotube [1] (**Figure 1**). This is achieved by a supply of two sets of six heptagonal defects onto both sides of the given nanotube. There exists the restrictions on the form of the nanotube—the chirality must be $(6n, 6n)$ armchair or $(6n, 0)$ zigzag and a radius of the nanotube is larger than its length.

The metric tensor of the wormhole is given by

$$g_{\mu\nu} = \Lambda^2(r_{\pm}) \begin{pmatrix} 1 & 0 \\ 0 & r_{\pm}^2 \end{pmatrix}, \quad \Lambda(r_{\pm}) = (a/r_{\pm})^2 \theta(a - r_{\pm}) + \theta(r_{\pm} - a), \quad (1)$$

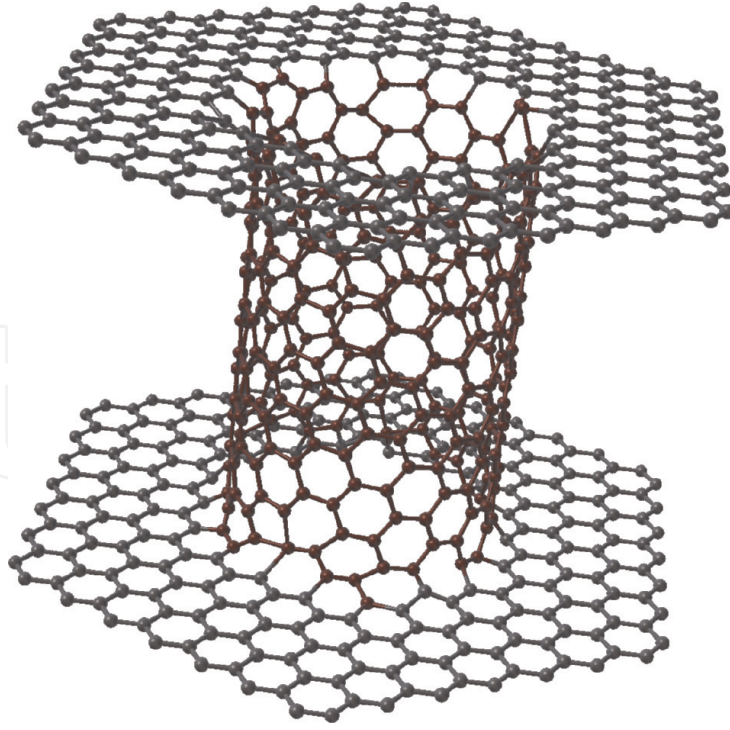


Figure 1.
Schematic representation of graphitic wormhole consisting from two graphene sheets connected together with the help of a nanotube.

where θ is the Heaviside step function, r_- and r_+ are the polar coordinates of lower and upper graphene sheets, and $a = \sqrt{r_- r_+}$ is the radius of the wormhole.

1.1 Electronic structure

We consider the continuum gauge field theory, i.e., at each point of a molecular surface, we take into account an influence of different gauge fields that enter the Dirac-like equation for an electron

$$i v_F \sigma^\mu \left[\partial_\mu + \Omega_\mu - i a_\mu - i a_\mu^W - i A_\mu \right] \psi = E \psi, \quad (2)$$

with σ^α matrices as the Pauli matrices, the Fermi velocity v_F , the spin connection

$$\Omega_\mu = \frac{1}{8} \omega_\mu^{\alpha\beta} [\sigma_\alpha, \sigma_\beta], \quad (3)$$

and the covariant derivative $\nabla_\mu = \partial_\mu + \Omega_\mu$. The gauge fields a_μ, a_μ^W are caused by the presence of the defects, and by rotational symmetry, the gauge field A_μ characterizes the possible magnetic field.

In the case of the wormhole with the metric Eq. (1), the effective flux caused by the presence of the defects is included in the gauge field a_μ , and for the particular polar components, it has the values $a_\varphi = \frac{3}{2}, a_r = 0$ for two possibilities: the first corresponds to the chiral vector with the form $(6n, 6n)$, the second corresponds to the chiral vector with the form $(6n, 0)$ and n divisible by 3. In the case of chiral vector of the form $(6n, 0)$, where n is not divisible by 3, the components of the gauge field are $a_\varphi = \frac{1}{2}, a_r = 0$. Regarding that the components of the spin connection are

$$\Omega_\varphi = -\frac{i}{2}\sigma_3\left(r\frac{\Lambda'(r)}{\Lambda(r)} + 1\right), \quad \Omega_r = 0, \quad (4)$$

and after the substitution into Eq. (2), we get the equation

$$iv_F\sigma^\mu(\partial_\mu + \Omega_\mu \mp i a_\mu)\psi^\pm = \varepsilon\psi^\pm, \quad (5)$$

where each sign corresponds to a different Dirac point

$$\begin{aligned} -iv_F\left(\partial_r + \frac{1}{r}i\partial_\theta \mp \frac{a_\varphi}{r} + \frac{1}{2r}\right)\psi_B^\pm &= \varepsilon\psi_A^\pm, \\ -iv_F\left(\partial_r - \frac{1}{r}i\partial_\theta \pm \frac{a_\varphi}{r} + \frac{1}{2r}\right)\psi_A^\pm &= \varepsilon\psi_B^\pm \end{aligned} \quad (6)$$

for $r \geq a$ and

$$\begin{aligned} iv_F\left(\frac{r}{a}\right)^2\left(\partial_r - \frac{1}{r}i\partial_\theta \pm \frac{a_\varphi}{r} - \frac{1}{2r}\right)\psi_B^\pm &= \varepsilon\psi_A^\pm, \\ iv_F\left(\frac{r}{a}\right)^2\left(\partial_r + \frac{1}{r}i\partial_\theta \mp \frac{a_\varphi}{r} - \frac{1}{2r}\right)\psi_A^\pm &= \varepsilon\psi_B^\pm \end{aligned} \quad (7)$$

for $0 < r \leq a$. For $r \geq a$, the solution is

$$\begin{aligned} \psi^\pm &= \begin{pmatrix} \psi_A^\pm(r, \varphi) \\ \psi_B^\pm(r, \varphi) \end{pmatrix} = c_1 \begin{pmatrix} J_{n \mp a_\varphi - 1/2}(kr) \\ -i \operatorname{sgn} \varepsilon J_{n \mp a_\varphi + 1/2}(kr) \end{pmatrix} \\ &+ c_2 \begin{pmatrix} Y_{n \mp a_\varphi - 1/2}(kr) \\ -i \operatorname{sgn} \varepsilon Y_{n \mp a_\varphi + 1/2}(kr) \end{pmatrix}, \end{aligned} \quad (8)$$

where the energy $\varepsilon = \pm v_F k$, $J_n(x)$ and $Y_n(x)$ are the Bessel functions.

The zero modes solve the Dirac equation for zero energy. If one choose the component ψ_A^\pm of the solution to be equal to zero, one get from (6) and (7)

$$\left(\partial_r - \frac{1}{r}i\partial_\theta \mp \frac{a_\varphi}{r} + \frac{1}{2r}\right)\psi_B^\pm = 0 \quad (9)$$

for $r \geq a$ and

$$\left(\partial_r - \frac{1}{r}i\partial_\theta \pm \frac{a_\varphi}{r} - \frac{1}{2r}\right)\psi_B^\pm = 0 \quad (10)$$

for $0 < r \leq a$. For ψ_B^- and the value $a_\varphi = \frac{3}{2}$, the solution is

$$\psi_B^-(r, \varphi) \sim r^{-n-2}e^{in\varphi} \quad (11)$$

for $r \geq a$ and

$$\psi_B^-(r, \varphi) \sim r^{-n+2}e^{in\varphi} \quad (12)$$

for $0 < r \leq a$. For both cases, it is normalizable only for $n = 0$, and so this is the only solution. In a similar way, we can calculate the zero modes for the component ψ_B^+ . For the value $a_\varphi = \frac{1}{2}$, possible solutions are not strictly normalizable, and the

zero modes exist only for the case of the connecting nanotube being armchair or zigzag with the chiral vector $(6n, 0)$, n divisible by 3. In other cases the zero modes do not exist.

Recently, in work [2] some peculiarities in the bilayer graphene were analytically predicted. A possible indication of the wormhole could be found in [3, 4], where a new type of zero modes is investigated. These zero modes could be the zero modes studied in this subsection applied to the case of the smallest wormhole.

1.2 Case of massive fermions

Up to now we supposed that the fermions appearing in the Dirac equation have the zero mass or that the mass is very small in comparison with their energy, but in [5, 6] it was shown that the Fermi velocity needs to be renormalized due to the elasticity and deformations in a graphene. In our case of the graphitic wormhole, including big deformations, the velocity of fermions close to the wormhole bridge could achieve such values that the relativistic effects can appear or break off the symmetry [7] and the mass of fermions would be non-negligible. The radius of the wormhole and its bridge is very small in comparison with the size of the upper and the lower graphene sheet (**Figure 2**) and by folding the sheet into a tube they acquire nonzero effective mass as they move along the tube axis. This change of the space topology of graphene from 2D to 1D space compactification is similar to the string theory compactification, and we can imagine a wormhole connecting nanotubes as 1D object.

To include the mass into the Dirac Eq. (2), one can transform the system of equations [8] into the differential equation of the second order

$$\left(\partial_{\xi\xi} - \frac{1}{2g_{\xi\xi}} \partial_{\xi} g_{\xi\xi} + \frac{\tilde{j}}{2} \sqrt{\frac{g_{\xi\xi}}{g_{\varphi\varphi}^3}} \partial_{\xi} g_{\varphi\varphi} - \tilde{j} 2 \frac{g_{\xi\xi}}{g_{\varphi\varphi}} + E^2 g_{\xi\xi} \right) u_j = 0. \quad (13)$$

One can suppose cylindrical geometry in order to simplify the equation into

$$\left(\partial_{\xi\xi} + E^2 - \frac{\tilde{j}^2}{R^2} \right) u_j = 0, \quad (14)$$

if a radius vector of the point at the surface will have the form

$$\vec{R} = (R \cos \varphi, R \sin \varphi, \xi), \quad (15)$$

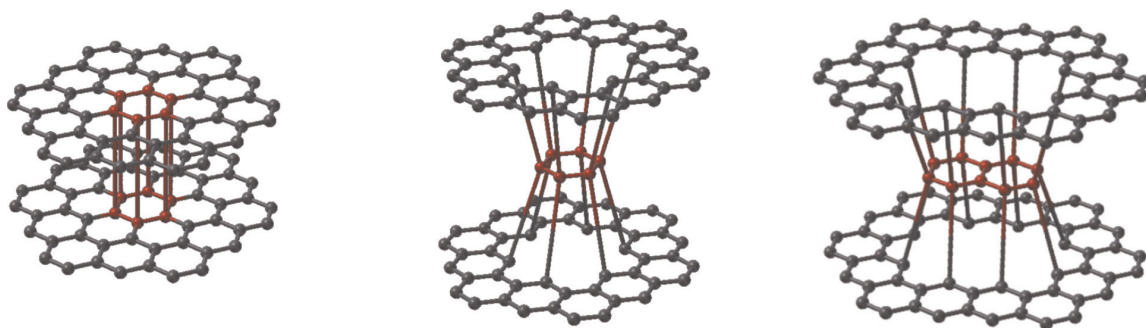


Figure 2.
The simplest realization of smallest graphitic wormholes.

with R as the radius of the cylinder. The solution of this equation has the form

$$u_j(\xi) = Ae^{k\xi} + Be^{-k\xi}, \quad k = \sqrt{\frac{\tilde{j}^2}{R^2} - E^2}. \quad (16)$$

A similar form has the dispersion relation associated with the massive 1D Dirac equation

$$k = \sqrt{M^2 - E^2}, \quad (17)$$

where M is the mass of corresponding fermion. It is proven [9] that for a suitable choice of the parameters, 2D massless case is in analogy with 1D massive case, and one can rewrite Eq. (13) in the form

$$\left(\partial_{\xi\xi} - \frac{1}{2g_{\xi\xi}} \partial_{\xi} g_{\xi\xi} + \frac{\tilde{j}}{2} \sqrt{\frac{g_{\xi\xi}}{g_{\varphi\varphi}^3}} \partial_{\xi} g_{\varphi\varphi} - \tilde{j} 2 \frac{g_{\xi\xi}}{g_{\varphi\varphi}} + (E^2 - M^2) g_{\xi\xi} \right) u_j = 0, \quad (18)$$

where M is the mass of the corresponding fermion. For different values of M , one can find the corrections of local density of states for the graphitic wormhole. It seems that these massive particles arising in the wormhole nanotubes could create energy bulks on and near the wormhole bridge which should be experimentally measured by the STM or Raman spectroscopy [10]. Another possibly identification of wormhole structure comes from the fact of creation of strain solitons and topological defects by massive particles on the bridge of bilayer graphene which should propagate throughout the graphene sheet. These are almost macroscopic effects and should be caught by the experimental physicists [11].

1.3 Spin-orbit coupling in the wormhole connecting nanotube

An important measurable quantity in carbon nanostructures, which includes a nanotubular part of a graphitic wormhole, is a spin-orbit coupling (SOC) [12, 13]. If one considers this influence, two-component Dirac equation could be changed into the usual four-component form, and as a consequence chiral fermions should be detected close to the wormhole bridge.

One can reflect on two sources of SOC: (1) the interatomic one that preserves the z -component of a spin and (2) so-called Rashba-type coming from the external electric field, which conserves the z -component of an angular momentum J_z . In both cases, the strength of SOC is influenced by the nonzero curvature. In the next we will be interested in the first source of the SOC.

Considering the SOC we can write the Dirac equation for the nanotube in the form

$$\hat{H} \begin{pmatrix} F_A^K \\ F_B^K \end{pmatrix} = \begin{pmatrix} 0 & \hat{f} \\ \hat{f}^\dagger & 0 \end{pmatrix} \begin{pmatrix} F_A^K \\ F_B^K \end{pmatrix} = E \begin{pmatrix} F_A^K \\ F_B^K \end{pmatrix}, \quad (19)$$

where

$$F_A^K = \begin{pmatrix} F_{A,\uparrow}^K \\ F_{A,\downarrow}^K \end{pmatrix}, \quad F_B^K = \begin{pmatrix} F_{B,\uparrow}^K \\ F_{B,\downarrow}^K \end{pmatrix}. \quad (20)$$

The expression \hat{f} has the following form

$$\hat{f} = \gamma(\hat{k}_x - i\hat{k}_y) + i\frac{\delta\gamma'}{4R}\hat{\sigma}_x(\vec{r}) - \frac{2\delta\gamma p}{R}\hat{\sigma}_y, \quad (21)$$

where

$$\hat{k}_x = -i\frac{\partial}{R\partial\theta}, \quad \hat{k}_y = -i\frac{\partial}{\partial y}, \quad \hat{\sigma}_x(\vec{r}) = \hat{\sigma}_x \cos\theta - \hat{\sigma}_z \sin\theta. \quad (22)$$

Next one can take

$$\gamma = -\frac{\sqrt{3}}{2}aV_{pp}^\pi, \quad \gamma' = -\frac{\sqrt{3}}{2}a(V_{pp}^\sigma - V_{pp}^\pi), \quad p = 1 - \frac{3\gamma'}{8\gamma}, \quad (23)$$

where a is the length of the atomic bond and V_{pp}^σ , V_{pp}^π are the hopping integrals for the σ and π bond, respectively.

For the interatomic source of the SOC, one has

$$\delta = \frac{\Delta}{3\epsilon_{\pi\sigma}}, \quad \Delta = i\frac{3\hbar}{4m^2c^2} \left\langle x_l \left| \frac{\partial V}{\partial x} \hat{p}_y - \frac{\partial V}{\partial y} \hat{p}_x \right| y_l \right\rangle \quad (24)$$

with the difference of energies of the relevant π and σ orbitals

$$\epsilon_{\pi\sigma} = \epsilon_{2p}^\pi - \epsilon_{2p}^\sigma, \quad (25)$$

x_l , and y_l being the local coordinates. By applying the transformation

$$\hat{H}' = \hat{U}\hat{H}\hat{U}^{-1}, \quad \hat{U} = \begin{pmatrix} \exp\left(i\hat{\sigma}_y \frac{\theta}{2}\right) & 0 \\ 0 & \exp\left(i\hat{\sigma}_y \frac{\theta}{2}\right) \end{pmatrix} \quad (26)$$

the transformed Hamiltonian \hat{H}' will have the form with two terms, including the \hat{H}_{SOC} term which corresponds to the spin-orbit coupling

$$\hat{H}' = \hat{H}_{kin} + \hat{H}_{SOC}, \quad \hat{H}_{kin} = -i\gamma \left(\partial_y \text{Id}_2 \otimes \hat{s}_y + \frac{1}{R} \partial_\theta \text{Id}_2 \otimes \hat{s}_x \right), \quad \hat{H}_{SOC} = \lambda_y \hat{\sigma}_x \otimes \hat{s}_y - \lambda_x \hat{\sigma}_y \otimes \hat{s}_x. \quad (27)$$

The operators $\hat{s}_{x,y,z}$ are the Pauli matrices, which transform the wave function of the A sublattice into the wave function of the B sublattice and vice versa.

In our model, the SOC is induced by the curvature, and it is described with the help of two strength parameters, namely, λ_x and λ_y in the form

$$\lambda_x = \frac{\gamma}{R} \left(\frac{1}{2} + 2\delta p \right), \quad \lambda_y = -\frac{\delta\gamma'}{4R}, \quad (28)$$

for the case of single-wall carbon nanotube with different magnitude. Here, $|\lambda_y| \ll |\lambda_x|$ and for $R \rightarrow 0$, both strengths go to infinity. So reminding the previous results, the chiral massive fermions should be detected around the wormhole bridge. For more complicated forms as perturbed nanotube in the wormhole center,

the geometry of the corresponding graphene sheets will be curved, and this brings a significant change of the physical properties.

1.4 Graphene black hole

The effects connected with the deformation of a graphene and a consequent change of the distance of the carbon atoms in the layer are described in [14]. It causes the rotation of the p_z orbitals and rehybridization of the π and σ orbitals. The procedure leads to the creation of the $p - n$ junctions similarly to the case of a transistor. This effect changes the Fermi level which is rising in the far areas from the wormhole center. The electron flux is directed from these areas to the middle where the electric charge is accumulated, and in the case of the deformed wormhole, one can speak about so-called graphene black hole. The form of a middle part of the nanotube plays a big role for this purpose. It cannot be unperturbed because in such a case the effect of the black hole would be disrupted. It can be ensured only in the case when the nanotubular neck is tapering in the direction to its center, because this ensures the decrease of the Fermi level [15]. The related effects which appear on the nanostructures are also described in [16], where the special relativistic-like properties of the Beltrami pseudosphere naturally point to quantum field theory in curved space. In the work the finite temperature local density of states is predicted that is a realization of the Hawking-Unruh effect. Mentioned effect of the graphene black hole could eventually disappear in the presence of external magnetic (electric) field which would cause the transfer of the charge from one wormhole sheet to another one through a nanotube center. This serves as an important model for further investigations of the electron flux in the presence of the defects with the applications in cosmological models.

2. Spinor fields in biological systems

One of the present problems in genetic engineering is the prediction of biological gene variation and the representation of corresponding genetic code. This issue emerges in the plotting graphs related to the connection curvature of a docking processes. The docking process is important in the genes of the protein structure and could be adopted instead of using a very long alphabet notation as the string sequence and the comparison of the sequences of docking. From this point of view, methods of quantum field theory, general relativity, and related tools can be of high interest. The equilibrium between the supersymmetry and the mirror symmetry of the left-handed and right-handed DNA, RNA, nucleic and amino acid molecules can be explained by anti-de Sitter (AdS) correspondence in the Yang-Mills theory and the Chern-Simon currents in biology as the curvature of the spectrum in genetic code of the protein curvature.

Today, a genetical structure is studied by standard alphabet codes A , T , C , G , and U as a sequence of strings for the representation of genetic code for various organisms without any exact definition of a new time series of genetic code [17] in contrast to standard time series modeling. With this representation [18], it is very difficult to calculate the genetic variation [19] and to perform calculations within a framework of self-consistent mathematical theory [20], namely, in the context of string theory and M- and G-theories [21, 22].

There are still attempts to perform empirical data analysis of the genetic variation [23] and to detect the pattern matching over the gene sequence by using algorithm over a standard alphabet code as their time series representation. It seems

that one main problem in this field is how can we predict the genetic variation and the gene structure in the viral particle and other organisms, or in the context of new representation, the question is how we can explain the intuition behind a definition of new time series data of gene, e.g., involved in the Batalin-Vilkovisky cohomology of DNA and the viral gene structure. The Chern-Simons current and the anomaly over a superspace of cell membrane can be applied to diagnose new gene diseases, the cloning technology or the gene therapy in medicine. Moreover, a presented method can be improved also in view of describing a useless trash area of DNA, which is considered as unknown part of human genome.

On the other side, another approach based on the usage of a spinor field in the Kolmogorov space of the time series data [24] over the genetic code can represent the gene structure as the ghost and anti-ghost fields of the codon and anticodon. This can be achieved in the frameworks of supersymmetry [25] and G-theory [22]. Results of the works show that all calculations over the codon can be assumed as a new superspace of the time series representation of the gene structure [24].

In [26–28], we introduced a new representation of the genetic code in the time series using a modeling by strings and D-branes. By applying a spinor field to a superspace in time series data [29], the method allows us to develop supersymmetry for living organisms. In particular, it is possible to control the anomalies in the codon and anticodon ghost fields and construct an algebraic approach for the trash DNA.

The “gravitational” analogy of the Chern-Simons currents in a gravitational physics, emanating from a system of DNA-RNA transcriptions, could have interesting counterparts also in biology. A representation of codons in human genome, derived from the Chern-Simons currents, can be useful in biology to explain the source of connections over protein-docking states. In this perspective, adopting cohomology in biology can be useful as a new modeling tool for plotting genes with spinor field in time series data. Especially, the junk area of DNA, with repeated inactive genes, can be represented by the Chern-Simons currents with extended structures of knot states in a Laurent polynomial of knots.

Further we discuss the role of spinors in the time series of genetic code. We can denote $\mathbb{H}P^1$ as a quaternionic projective space and $H_0(X_t)$ as a pointed space of DNA alphabet sequence with $[A]$, $[T]$, $[C]$, and $[G]$ as an equivalent class of $[A]$, $[T]$, $[C]$, $[G] \in H_0(X_{t,DNA}) := \Phi_i(X_t)$ a ghost field with parity two with $H_0(X_t) = H_0(X_t, *)$ where $*$ = $\{*\}$ is a pointed space. We define an equivalent class of DNA–RNA translation processes by using the notation of a master equation for an interaction between the viral RNA and the host cell DNA by $\{x_t, y_t\} = \{DNA, RNA\}$. The whole state space model of the viral replication cycle, embedded in the host cell, is denoted by $X_{t,DNA}/Y_{t,RNA} = Z_{t,GENE} = \mathbb{H}/\mathbb{H} = \mathbb{H}P^1$ as a moduli state space model with the definition of genetic code as an equivalent class of the map $\alpha_t : X_{t,DNA} \rightarrow \{[A], [T], [C], [G]\} \subset \mathbb{H}$; the host cell gene alphabet is defined by a hidden state space X_t with the gene β_i

$$\begin{aligned} [A]_{DNA} &:= \left[e^{\frac{i\pi\beta_i}{2}} \right] + [0]\mathbf{i} + [0]\mathbf{j} + [0]\mathbf{k}, \\ [T]_{DNA} &:= [0] + \left[e^{-\frac{i\pi\beta_i}{2}} \right] \mathbf{i} + [0]\mathbf{j} + [0]\mathbf{k}, \\ [C]_{DNA} &:= [0] + [0]\mathbf{i} + \left[e^{i\pi\beta_i} \right] \mathbf{j} + [0]\mathbf{k}, \\ [G]_{DNA} &:= [0] + [0]\mathbf{i} + [0]\mathbf{j} + \left[e^{i2\pi\beta_i} \right] \mathbf{k}. \end{aligned} \tag{29}$$

In the retroviral RNA of the observed state space $Y_{t,RNA}$ is a span by gene α_i with the anti-ghost field $\Phi_{i,+}(Y_{t,RNA})$ of viral particle. We define a pair of ghost and anti-ghost field genes by a middle hidden state in mRNA and ribosomal EPA state in codon and anticodon state as the ghost and anti-ghost fields in the genetic code. One

can define a mutual genetic code as passive or dual hidden states $[s_1]^*$, ..., $[s_8]^*$ and active eight states $[s_1]$, ..., $[s_8]$ for the spinor field in the genetic code by

$$\begin{aligned} [A]_{tRNA} &:= [NU]_{mRNA} = \left[e^{\frac{j\pi\alpha_i}{2}} \right] + [0]\mathbf{i} + [0]\mathbf{j} + [0]\mathbf{k}, \\ [U]_{tRNA} &:= [NA]_{mRNA} := [0] + \left[e^{-\frac{j\pi\alpha_i}{2}} \right] \mathbf{i} + [0]\mathbf{j} + [0]\mathbf{k}, \\ [C]_{tRNA} &:= [NG]_{mRNA} := [0] + [0]\mathbf{i} + \left[e^{j\pi\alpha_i} \right] \mathbf{j} + [0]\mathbf{k}, \\ [G]_{tRNA} &:= [NC]_{mRNA} := [0] + [0]\mathbf{i} + [0]\mathbf{j} + \left[e^{j2\pi\alpha_i} \right] \mathbf{k}. \end{aligned} \quad (30)$$

The reversed transcription process of the gene expression is defined by a moduli state space model of a coupling spinor field between the gene of a viral particle and the host cell (**Figure 3**)

$$\mathbb{H}P^1 = X_t/Y_t \ni \left[1, \frac{e^{\frac{2^2_{ni}\alpha}}{2^4_{mj}\beta}} \right]_{m,n=1,2,3,4} = \left[1, \frac{q|_{DNA}}{q^*|_{RNA}} \right] = \left[\frac{q|_{DNA}}{q^*|_{RNA}}, 1 \right]. \quad (31)$$

One can define $Sp(1) \rightarrow S^7 \rightarrow \mathbb{H}P^1$ as a Hopf fibration of eight states of the genetic code $[s_1], [s_2], \dots, [s_8] \in S^7 = T_p \mathcal{M}$, denoted by $[s_1]^*, [s_2]^*, \dots, [s_8]^* \in T_p^* \mathcal{M}$ states of the genetic code of the space of a viral RNA X_t and a space of host cell DNA, Y_t .

If $\mathcal{U}_{[A]_\alpha} \subset \mathbb{H}P^1$ is a chart of local coordinate in a manifold of genetic code over X_t/Y_t , where $[A]_\alpha$ is defined over the right-hand isomer genetic code $\{A, T, C, G\}$ (for the simplicity we use a symbol G also for U) with their dual $[A]_\alpha^*$, with the mirror symmetry of a genetic code $\{NA, NT, NC, NG\}$. We have a cycle and a cocycle of an orbifold as a trivialization over the tangent of the living organism manifold, so-called codon and anticodon $\mathcal{U}_i \cap \mathcal{U}_j \cap \mathcal{U}_k$. Let (\mathcal{M}, g) be a living organism manifold with $\mathcal{M} = \mathbb{H}P^1$ for a living organism with the Riemannian metric tensor $g_{ij} = \langle T_{[A]_\alpha} \mathcal{M}, T_{[A]_\alpha}^* \mathcal{M} \rangle$ over a tangent manifold and a cotangent manifold

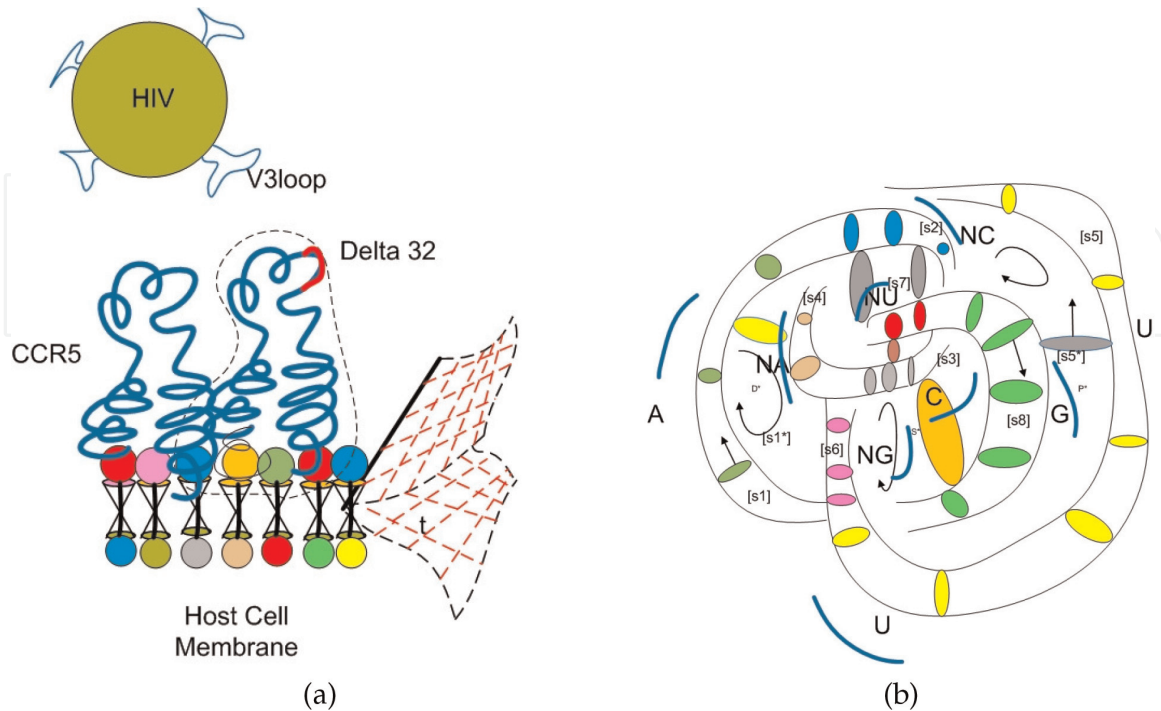


Figure 3.
 (a) The site of docking between CCR5 $\Delta 32$ co-receptor in host T-cell membrane and V3 loop in HIV viral gp120. The cell membrane has a mirror symmetry structure of D-brane for outer layer. The anti-D-brane structure of the cell membrane is an inner layer of phospholipid. (b) The knot 4_1 model of a short exact sequence of hidden eight states in genetic code.

$T_{[A]_a} \mathcal{M} = S^7$ with g_{ij} defined as a tensor behavior field transformation between 64 states in a codon as the distance in a space of the genetic code with $i, j = 1, 2, 3, \dots, 8$. The active states in genetic code are denoted as $[s_1], [s_2], \dots, [s_8]$, and the hidden states inside eight states or passive states are denoted as $[s_1^*], [s_2^*], \dots, [s_8^*]$. The dual part of a genotype $[s_i^*]$ is defined by a tangent of a manifold of the genetic code with the Jacobian $J = \sqrt{g_{ij}}$, where the metrics is $g_{ij} = \langle [s_i], [s_j]^* \rangle$. A smallest state in gene is defined as a pair of a genetic code by a classical notation $A - T, C - G$ with the coordinates $(A, T), (C, G)$. One can define a superstate in a pair of genes as ghost and anti-ghost fields in the genetic code with the supersymmetry of D-isomer to L-isomer from the right-hand D-state in the light of the polarization in a nucleic acid as $[s_i]_{\Phi_i}$ to a left-hand light L-state of an isomer of a light polarization, denoted as $[s_i]_{\Phi_i}^*$

$$\begin{aligned}
 [s_1] &= ([A], [T]^*) \in T_p \mathcal{M}, & [p1] &= [s_1]^* = [s_{11}]^* = ([A], [T]^*)^* \in T_p^* \mathcal{M} \\
 [s_2] &= ([A], [NA]) \in T_p \mathcal{M}, & [s_2]^* &= ([A], [NA])^* \in T_p^* \mathcal{M} \\
 [s_3] &= ([C], [G]^*) \in T_p \mathcal{M}, & [s_3]^* &= ([C], [G]^*)^* \in T_p^* \mathcal{M} \\
 [s_4] &= ([C], [NC]) \in T_p \mathcal{M}, & [s_4]^* &= ([C], [NC])^* \in T_p^* \mathcal{M} \\
 [s_5] &= ([T], [T]^*) \in T_p \mathcal{M}, & [s_5]^* &= ([T], [T]^*)^* \in T_p^* \mathcal{M} \\
 [s_6] &= ([T], [NA]) \in T_p \mathcal{M}, & [s_6]^* &= ([T], [NA])^* \in T_p^* \mathcal{M} \\
 [s_7] &= ([G], [G]^*) \in T_p \mathcal{M}, & [s_7]^* &= ([G], [G]^*)^* \in T_p \mathcal{M} \\
 [s_8] &= ([G], [NC]) \in T_p \mathcal{M}, & [s_8]^* &= ([G], [NC])^* \in T_p \mathcal{M}
 \end{aligned} \tag{32}$$

As known from biochemistry, there exist only $[s_1] = ([A], [T]^*)$ and $[s_3] = ([C], [G]^*)$ observational states of the living organism in nature. However, in the theory of supersymmetry of S^7 Hopf fibration, there exist eight states of the ghost fields with six hidden states in the mirror symmetry. In each state, an orbifold of the living organism, other eight states denoted p_1-p_8 exist. One can define all 64 states with the help of a notation for the Riemann tensor field $g_{ij} = \langle [s_i], [s_j]^* \rangle$, e.g., $g_{11} = \langle [s_1], [s_1]^* \rangle$, and we denote a pair of states in a gene as $([s_1], [p_1])$. It is a pair of the genetic code $g_{11} = \langle ([A], [T]^*), ([A], [T^*]) \rangle$; for the case of codon, we replace $[T]$ with $[U]$. Finally, we have for $g_{11} = \langle ([A], [[T]^*]), ([A], [T^*]) \rangle = \langle ([A], ([A], [T^*]) \rangle$ since the states $[T^*]$ are hidden states, so one has a codon AAU for g_{11} .

If $\Gamma_{ij}^k := [A]_k$ is a connection over a tangent of a manifold of X_t/Y_t with $\mathcal{M} = \mathbb{H}P^1$ of the genetic code $k \in \{A, T, C, G\}$, one can denote $\Gamma_{\mu\nu}^k := F_{\mu\nu}$ as the behavioral Yang-Mills field with its dual in AdS theory of supersymmetry with $*F_{\mu\nu} = F^{\mu\nu}$. It is a behavior of a protein folding inducing a curvature between a viral glycoprotein and a host cell receptor. The behavior of a Yang-Mills field is an interaction field between the behavior of virus and host cells which can survive by a change of curvature of the protein during the evolution. It is a connection in the sense of an evolutionary field not in the sense of traditional gravitational field as usual

$$\Gamma_{ij}^k = \frac{1}{2} g^{kl} \left(\partial_j g_{jk} + \partial_i g_{jk} - \partial_k g_{jk} \right), \tag{33}$$

where $g_{ij} = \langle [s_i], [s_j]^* \rangle$.

For an equilibrium state of evolution of an organism, we have no change of covariant derivative for the tensor field g

$$\nabla_g g = 0. \quad (34)$$

We can define a $F^{\mu\nu} := (A_\alpha)_\mu^\nu$ as a connection on a principle bundle $Sp(1) \rightarrow S^7 \rightarrow \mathbb{H}P^1$ of a genetic code over a supermanifold of a viral particle \mathcal{A} . We can use an exact sequence of the sheave cohomology \mathcal{O}_{X_t} with the chart over the supermanifold defined by homogeneous coordinates of $\mathbb{H}P^1$ for viral gene X_t along the host cell gene \mathcal{O}_{Y_t} , while the virus attachment to the host cell is defined by the coordinate in sheave \mathcal{O}_{X_t/Y_t} . We apply a supersymmetry AdS theory over a Yang-Mills field of a behavioral field of the genetic code as a connection over $(A_\alpha) \in \{[A], [T], [C], [G]\} \subset \mathbb{H}P^1$ with the Hopf fibration of viral RNA gene $F^{\mu\nu} := (A_\alpha)_\nu^\mu = \Gamma_{\alpha\nu}^\mu$ with an anti self dual field over the gene of the host cell DNA, $*F_{\mu\nu}$. A current J of the connection between the fields is defined by the Chern-Pontryagin density for the interaction of behavioral fields. The current varies from the curvature of docking between the behavior of the curvature over amino acid k in X_t and its dual curvature in Y_t while docking $\langle F^{\mu\nu} * F_{\mu\nu} \rangle$, where $\langle - \rangle$ is an average or an expectation operator.

The connection between genes is

$$R_{\nu\alpha\beta}^\mu = \partial_\alpha (A_\beta)_\nu^\mu - \partial_\beta (A_\alpha)_\nu^\mu + [A_\alpha, A_\beta]_\nu^\mu, \quad (35)$$

where $R_{\nu\alpha\beta}^\mu$ is the curvature over a tangent space of a genetic code $(A_\alpha) \in \{[A], [T], [C], [G]\} \subset \mathbb{H}P^1$ and $(A_\alpha)_\nu^\mu := \Gamma_{\alpha\nu}^\mu = F^{\mu\nu}$ is the connection of the coupling between two alphabets of two organisms, i.e., from DNA and viral RNA. The above curvature is also useful in other situations like t-RNA docking with DNA in interaction between two D-branes of DNA and RNA. In a gauge field theory of DNA and RNA genetic codes of translation process, it is the group action of Lie-algebra one form. We have an adjoint representation of the genetic code as a translation process over the codon and anticodon of $t - RNA$. One needs to define a new value to measure the curvature in amino acids of protein structure, not in the tangent space of a genetic code, and one needs to define a curvature over the codon and anticodon to represent a curvature of proteins while they are docking. The new value needs to be unique for all states in the codon and to have a meaning of curvature of genetic code with connection over manifold of genetic code. To represent a spectrum of genetic variation as curvature in protein structure while docking, one can introduce a new quantity, so-called Chern-Simons current for biology.

One can translate a genetic code in a codon in three steps. The translation operator of group is given by a behavior matrix in Lie group, a group of supermanifold of living organism with action in three times. It generates a codon representation as an adjoint representation over gene expression, and it is a precise definition of genetic code with parity two of ghost field and anti-ghost field in the Chern-Simons current for the representation of a gene A_i with the current density $J^{A_i} = \int_{t_1}^{t_2} dJ^{A_i}$.

Let a knot serve as a representation of anticodon in t-RNA topological structure for amino acid μ with J^μ as a representation R of gauge group G of gene geometric translation as group action of transcription process; then the genetic code is an average expectation value of Wilson loop operator of coupling between hidden state of x_t and y_t twist D-brane and anti-D-brane over superspace of cell membrane, i.e.,

$$W(K, R) = \text{Tr}_R P \exp (\oint_K A). \quad (36)$$

The above term gives the asymmetric property of chiral molecule of DNA and RNA, twisted from the left hand to the right hand in a supersymmetry breaking as knot polynomial related to the connection A . By such a way, we can represent the genetic code as Laurent polynomials in variable q with integer coefficients, and for any knot K we have

$$J(K, q) = \sum_{i=1}^n a_n q^n. \quad (37)$$

By using the new parameter of knot q

$$q = e^{\frac{2\pi}{k+h}} \quad (38)$$

one can induce a spinor field for representation of genetic code, where h is the dual coexter number for group action of supersymmetry of gene expression G . It might be the source of evolution from the adaptive behavior derived from the environment. In the next, we set $h = 0$ in our definition of the Chern-Simons current for biology for the simpler derivation of formulas.

A Chern-Simons current J^μ for anomaly quantum system of codons can be also defined as the spectrum of curvature in the genetic code for gene evolution detection. Under the definition we mean a differential 3-forms in cohomology of spin fiber S^3 over the homotopy class $[S^3, X_t/Y_t]$ in the codon of t-RNA molecule. A path integral of gene expression is defined by the Chern-Simons theory over knots of codon and anticodon: it is defined by the interaction between codon A_i and anticodon between DNA and RNA in the form of integral $A_i + S_{CS} = \int \mathcal{D}A_i \exp (iS_{CS})$

$$S_{CS} = \frac{k}{4\pi} \int_W \text{Tr} \left(A \wedge dA + \frac{2}{3} A \wedge A \wedge A \right) \quad (39)$$

and

$$\begin{aligned} J(q; K^{A_i}, R_i) &= \langle W(K_i, R_i) \rangle \\ &= \langle \text{Tr}_{R_i} P \oint_{K_i} A \rangle = \frac{\int \mathcal{D}A_i \exp (iS_{CS}) \Pi_i W(K_i, R_i)}{\int \mathcal{D}A_i \exp (iS_{CS})}. \end{aligned} \quad (40)$$

The explicit definition of curvature over the connection of genetic code has also new meaning of the genetic spectrum current J^μ , $\mu = 1, 2 \dots 20$ of the Chern-Simons current; it is generated from the representation of Lie group over manifold of a host cell.

An example of our approach can serve as a case of phenylalanine (*Phe*), where UUU and UUC definition is

$$\begin{aligned} J^{Phe} &= e^{\mu\alpha\beta\alpha} \left\langle \frac{1}{2} A_\alpha \partial_\beta A_\gamma + \frac{1}{3} A_\alpha A_\beta A_\gamma \right\rangle \\ &= e^{\mu\alpha\beta\alpha} \left\langle \frac{1}{2} (A_2)_\nu^\mu d(A_2)_\nu^\mu + \frac{1}{3} (A_2)_\nu^\mu (A_2)_\nu^\mu (A_2)_\nu^\mu \right\rangle \end{aligned} \quad (41)$$

where we explicitly define the differential form of genetic code for *Phe* by $dA_2 = A_2 A_2 - A_2 A_3 := UU - UC$, so we have

$AdA = A_2(A_2A_2 - A_2A_3) = A_2A_2A_2 - A_2A_2A_3$. The minus sign represents a linear combination of basis for codon. Therefore it follows

$$\begin{aligned} J^{Phe} &= \epsilon^{\mu\alpha\beta\gamma} \left\langle \frac{1}{2} A_\alpha \partial_\beta A_\gamma + \frac{1}{3} A_\alpha A_\beta A_\gamma \right\rangle \\ &= \int \text{Tr} \left(\frac{5}{6} U \wedge U \wedge U - \frac{1}{2} U \wedge U \wedge C \right) = \int \text{Tr}(H^3(\mathcal{M})). \end{aligned} \quad (42)$$

For a translation in reversed direction of antigen shift and drift in gene evolution theory, we can use the definition of the group action of reversed direction of time by the *CPT* theory for anti-ghost field in field of time series of antibody gene as

$$\begin{aligned} \{x_t, y_t\} &= \int \text{Tr}(H^3(\mathcal{M})) = \sum_{i=1}^3 g^i(x_t/y_t) \\ &= \alpha_t y_t, g^3 x_t/y_t \rightarrow \beta_t x_t/\alpha_t y_t \simeq [\epsilon_t^*] = \int \text{Tr} H^3(\mathcal{M}, g, F^{\mu\nu}). \end{aligned} \quad (43)$$

Then a numerical representation for spinor field of curvature in the gene expression by the Chern-Simons action is defined as follows:

$$S_{CS} = \frac{k}{4\pi} \int \text{Tr} \left(A \wedge dA + \frac{2}{3} A \wedge A \wedge A \right) \quad (44)$$

where $k = 1, 2, 3, \dots, n$ are

$$J^{\text{Amino}} = J^k \simeq \sqrt{\frac{2}{k+2}} \sin \frac{\pi}{k+2} = \int D[A]^{S_{CS}}. \quad (45)$$

The derivation of the Chern-Simons current can be done by a simple algorithm [30], i.e., the Chern-Simons current maps the string of genetic code into numerical values by explicit formulas. It can be used to plot the time series data directly into the superspace of gene expression. We transform the alphabet string values, which cannot be computed in the classical standard definition of genetic code, into the Chern-Simons current of time series data of genetic code with $k = 1, 2, 3, \dots, 64$ over spinor field with ground field of real values. We think that the approach is more suitable for computational programs used in data analyses.

3. Circular Artin braid group representation for spinor field in genetic code

In each cell division, the telomeres are shortened [31], and total length of DNA is changing. As the result of shorter biological clock from cell division, the living things die. In order to understand cell cocycle and division mechanism of telomerase aging, one can explain the source of cancer as a source of age acceleration and its relationship to telomere shortening mechanism. It is a source of braid group operation [32] so-called self-diffeomorphism in the genetic code. The age acceleration is a relative measurement between the chronical clock and the biological clock in telomere. Up to now, scientists understand that a telomere and telomerase are the locations of ancient viruses that rely on DNA in the chromosomes of living organisms. Telomere is composed of the repeated sequence of $(TTAGGG)_{dt^*}$ where

$1000 \leq dt^* \leq 2000$. The size of the duplicate sequence at the end of this open chromosome is amplified by six braids caused by six superspaces in time series data of organisms. The G alphabet might be suitable to be chosen as hidden time scale in the biological clock.

Here we assume that all genetic code cannot be completely separated and biological clock in telomere length is parametrized by a hidden state of the number of $dt^* := [G]$ alphabet in $(TTAGGG)_{n=dt^*}$ repeated pattern of the telomere. The element is Grothendieck topology over an adjoint cofunctor; it is a self-diffeomorphism $\xi : B_3^c \rightarrow B_3^c$. The loop braid generator for B_3^c is a quaternionic field in genetic code. We define their explicit forms and their permutations over the symmetric group by a chosen basis in Clifford algebra as

$$\sigma_D \rightarrow \left[\frac{1}{2}, \frac{1}{2}, -\frac{1}{2} \right], \quad \sigma_R \rightarrow \left[-\frac{1}{2}, \frac{1}{2}, \frac{1}{2} \right], \quad \sigma_P \rightarrow \left[\frac{1}{2}, -\frac{1}{2}, \frac{1}{2} \right], \quad (46)$$

and $\sigma_{D^*} = \sigma_D^{-1}$, $\sigma_{R^*} = \sigma_R^{-1}$, and $\sigma_{P^*} = \sigma_P^{-1}$. We have

$$\sigma_{D^*} \rightarrow \left[-\frac{1}{2}, -\frac{1}{2}, \frac{1}{2} \right], \quad \sigma_{R^*} \rightarrow \left[\frac{1}{2}, -\frac{1}{2}, -\frac{1}{2} \right], \quad \sigma_{P^*} \rightarrow \left[-\frac{1}{2}, \frac{1}{2}, -\frac{1}{2} \right], \quad (47)$$

therefore one can write eight bases for spinor field in the genetic code in braid form as follows

$$\begin{aligned} \sigma^{[G]} &:= [0, 0, 0] \sigma_R^{-1} \sigma_D = \sigma_R^{-1} \sigma_D, \\ \sigma^{[A]} &:= [0, 0, 1] \sigma_R^{-1} \sigma_D = (\sigma_D \sigma_R) (\sigma_R^{-1} \sigma_D), \\ \sigma^{[U]} &:= [0, 1, 0] \sigma_R^{-1} \sigma_D = (\sigma_P \sigma_D) (\sigma_R^{-1} \sigma_D), \\ \sigma^{[C]} &:= [1, 0, 0] \sigma_R^{-1} \sigma_D = (\sigma_R \sigma_P) (\sigma_R^{-1} \sigma_D), \\ \sigma^{[NA]} &:= [0, 1, 1] \sigma_R^{-1} \sigma_D = (\sigma_R \sigma_P) (\sigma_P \sigma_D) (\sigma_R^{-1} \sigma_D), \\ \sigma^{[NU]} &:= [1, 1, 0] \sigma_R^{-1} \sigma_D = (\sigma_D \sigma_R) (\sigma_R \sigma_P) \sigma_R^{-1} \sigma_D, \\ \sigma^{[NC]} &:= [1, 0, 1] \sigma_R^{-1} \sigma_D = (\sigma_P \sigma_D) (\sigma_D \sigma_R) (\sigma_R^{-1} \sigma_D), \\ \sigma^{[NG]} &:= [1, 1, 1] \sigma_R^{-1} \sigma_D = (\sigma_R \sigma_P) (\sigma_P \sigma_D) (\sigma_D \sigma_R) (\sigma_R^{-1} \sigma_D). \end{aligned} \quad (48)$$

We may also use $\theta = 2\pi s$ with spin quantum number s being an integer for retrotransposon and half-integer for geneon, so that

$$e^{i\theta} = e^{2i\pi s} = (-1)^{2s} \psi_2 \psi_1. \quad (49)$$

In a 3-dimensional position space, the geneon and retrotransposon statistics operators are -1 and $+1$, respectively. By the same way, in two-dimensional position space, the abelian anyonic statistics operators $e^{i\theta}$ are 1-dimensional representations of eight loop braid elements $\sigma_1, \sigma_1^2, \sigma_1^3, \dots, \sigma_1^8$ in circular Artin braid group B_2^3 acting on the space of wave functions (**Figure 4**).

3.1 Classification of loop braid group in genetic code

We classify three types of loop braid group operations; it is a representation of an anyon for protein folding. For two-dimensional representation of D-brane in loop braid group for the genetic code, we define abelian anyon for biology in $(2 + 1)$ dimensions, the extra dimensions used to represent the homotopy path of protein folding.

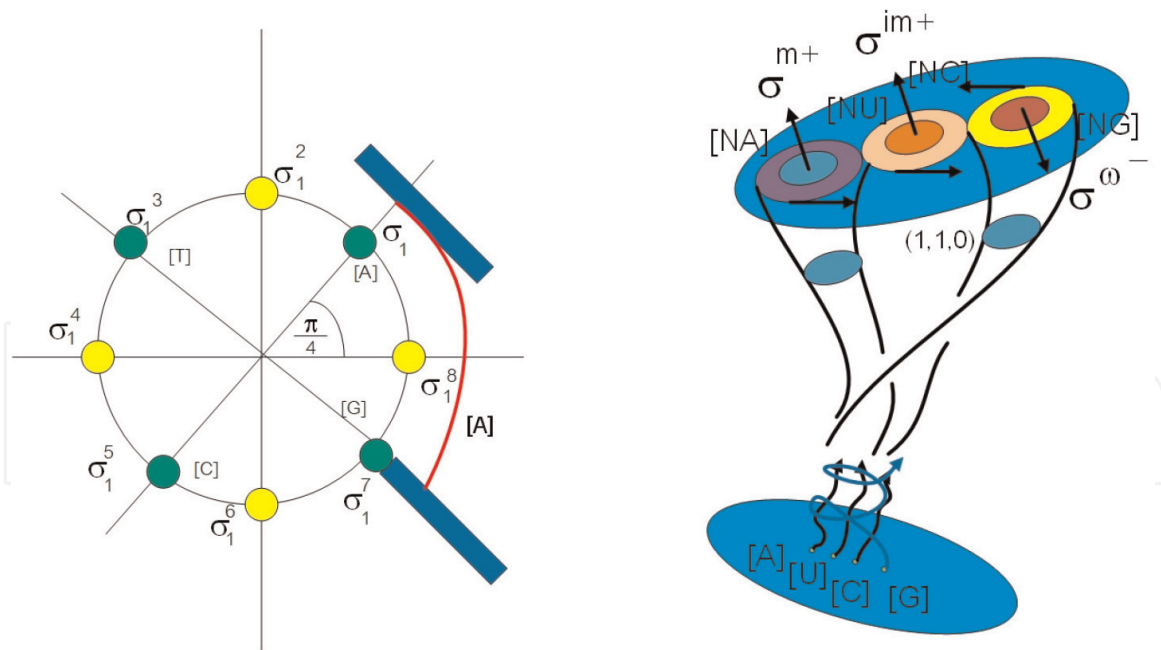


Figure 4.
 The left picture shows biological Artin braid element $\sigma_1 \in B_2$ in complex plane \mathbb{C} . There are eight equivalent classes span by eight orders of σ_1 . It is a representation of eight states in three genetic codes in codon as braid element in $(\sigma_1^{[A_\mu]}, \sigma_1^{[A_\mu]}, \sigma_1^{[A_\mu]}) \in B_2^3$. The red color line represents the curvature from the physiology of biological time series data, and the blue color represents the active and passive behavior field layers. The right picture shows a member of loop braid group. Three circles S^1 represent the sources of closed 3-balls B_3^c , the structure group of affine transform of 3 behavior fields in genetic code $\sigma_i^{[A_\mu]} \in B_2^3$ action on affine fibre bundle of behavior field in the genetic code $\sigma^{\omega^\pm}, \sigma^{im^\pm}, \sigma^{m^\pm} \in B_3^c$. We have affine group as loop braid group in genetic code by $B_2^3 \times B_3^c$.

The loop braid group, LB_n^{BIO} , for a genetic code has three types of generators, $\sigma = (\sigma_D, \sigma_R, \sigma_P)$, $\rho = (\sigma^{[A]}, \sigma^{[U]}, \sigma^{[C]}, \sigma^{[G]})$, and $\tau = (\sigma^\omega, \sigma^{im}, \sigma^m)$. The generators $\{\sigma_i, \rho_i \in B_2^3, i = 1, \dots, n-1\}$ and $\{\tau_i \in B_3^c, i = 1, \dots, n\}$ fulfill the relations

$$\begin{aligned}
 \tau_i \tau_j &= \tau_j \tau_i, & i &\neq j \\
 \tau_i^2 &= 1, & i &= 1, \dots, n \\
 \sigma_i \tau_j &= \tau_j \sigma_i, & |i - j| &> 1 \\
 \rho_i \tau_j &= \tau_j \rho_i, & |i - j| &> 1 \\
 \tau_i \rho_i &= \rho_i \tau_{i+1}, & i &= 1, \dots, n-1 \\
 \tau_i \sigma_i &= \sigma_i \tau_{i+1}, & i &= 1, \dots, n-1 \\
 \tau_{i+1} \sigma_i &= \rho_i \sigma_i^{-1} \rho_i \tau_i, & i &= 1, \dots, n-1.
 \end{aligned} \tag{50}$$

For a group operation of the genotype G and a representation ρ for gene translation as an anyon, we have $\rho : G \rightarrow U(1) = S^2$ as a representation in Ω_n^{BIO} and in LB_n^{BIO} . In order to visualize 3D folding structure of the protein structure, we define three types of loop braid group operations in biology. All loop elements of the representation of amino acids arose from group operations over the superspace of time series data. These tree types are a translation, reflection, and rotation, ρ^{Type-I} , $\rho^{Type-II}$, and $\rho^{Type-III}$. For the translation as a string of amino acids, we have the anyon *Type - I* for biology,

$$\begin{aligned}
 &\rho^{Type-I}(\sigma_i) \rho^{Type-I}(\sigma_{i+1}) \rho^{Type-I}(\sigma_i) \\
 &= \rho^{Type-I}(\sigma_{i+1}) \rho^{Type-I}(\sigma_i) \rho^{Type-I}(\sigma_{i+1}),
 \end{aligned}$$

$$\begin{aligned}
 & \rho^{\text{Type-I}}(\sigma_{i+1})\rho^{\text{Type-I}}(\sigma_i)\rho^{\text{Type-I}}(\sigma_{i+1}) \\
 & = \rho^{\text{Type-I}}(\sigma_{i+1})\rho^{\text{Type-I}}(\sigma_{i+1})\rho^{\text{Type-I}}(\sigma_i), \\
 & \rho^{\text{Type-I}}(\sigma_i) = \rho^{\text{Type-I}}(\sigma_{i+1}).
 \end{aligned} \tag{51}$$

It is isomorphic to the mapping class group of the infinitely punctured disk, a discrete set of punctures limiting to the boundary of the disk.

By an analogy with the action of the symmetric group by permutations in various mathematical settings, there exists a natural action of the braid group on n -tuples of objects or on the n -folded tensor product that involves some twistors. Let us consider an arbitrary group G , and let X be the set of all n -tuples of elements of G whose product is the identity element of G . The kernel of the homomorphism $LB_n^{\text{BIO}} \rightarrow \Omega_n^{\text{BIO}}$ is a subgroup of LB_n^{BIO} called pure loop braid group for biology on n strands and denoted as LP_n^{BIO} . In the pure braid, the beginning and end of each strand are in the same position. Pure braid groups fit into a short exact sequence

$$1 \rightarrow LF_{n-1} \rightarrow LP_n^{\text{BIO}} \rightarrow LP_{n-1}^{\text{BIO}} \rightarrow 1. \tag{52}$$

This sequence splits, and therefore pure braid groups are realized as iterated semi-direct products of free groups.

The braid group B_3 is the universal central extension of the modular group $PSL(2, \mathbb{Z})$, with these sitting as lattices inside the universal covering group. If we define \mathcal{O}_D , \mathcal{O}_R , and \mathcal{O}_P as active layers over the superspace of DNA, RNA, and protein, \mathcal{O}_{D^*} , \mathcal{O}_{R^*} , and \mathcal{O}_{P^*} , as passive layers, we can define braid group in genetic code by a curvature inside DNA, RNA, and protein folding structure. It is a source of an acceleration of biological clock in the epigenetic code. We let σ_D , σ_R , σ_P , σ_{D^*} , σ_{R^*} , σ_{P^*} , and $\sigma^{[A_\mu]}$ and $[A_\mu] = [A], [U], [C], [G], [NA], [NU], [NC], [NG]$ be a loop braid group elements in the genetic code. They are the circular Artin braid groups for the genetic code. One can then define

$$\Psi^R = \sigma_D \sigma_R \sigma_D, \quad \Psi^P = \sigma_D \sigma_R, \quad \Psi^{P^*} = \sigma_R \sigma_D \sigma_R. \tag{53}$$

The braid group operation gives Ψ^P

$$\sigma_D \Psi^P \sigma_D^{-1} = \sigma_R \Psi^P \sigma_R^{-1} = \Psi^P \tag{54}$$

implying that Ψ^P is in the center of B_3 . It is a wave function of protein transition anyon state. If $G = LB_n^{\text{BIO}}$ acts on X_t , we get

$$\begin{aligned}
 & \sigma_i^{D^*} \Psi_i(d_1, \dots, d_{i-1}, d_i, d_{i+1}, \dots, d_n) \\
 & = \Psi_i(d_1, \dots, d_{i-1}, d_{i+1}, d_{i+1}^{-1} d_i d_{i+1}, d_{i+2}, \dots, d_n).
 \end{aligned} \tag{55}$$

If $G = LB_n^{\text{BIO}}$ acts on Y_t , we get

$$\begin{aligned}
 & \sigma_i^{R^*} \Psi_i(r_1, \dots, r_{i-1}, r_i, r_{i+1}, \dots, r_n) \\
 & = \Psi_i(r_1, \dots, r_{i-1}, r_{i+1}, r_{i+1}^{-1} r_i r_{i+1}, r_{i+2}, \dots, r_n).
 \end{aligned} \tag{56}$$

If $G = LB_n^{\text{BIO}}$ acts on $P_t = X_t/Y_t$, we get

$$\begin{aligned}
 & \sigma_i^{P^*} \Psi_i(p_1, \dots, p_{i-1}, p_i, p_{i+1}, \dots, p_n) \\
 & = \Psi_i(p_1, \dots, p_{i-1}, p_{i+1}, p_{i+1}^{-1} p_i p_{i+1}, p_{i+2}, \dots, p_n).
 \end{aligned} \tag{57}$$

Thus the elements d_i and d_{i+1} exchange places in DNA strand by an analogy with genetic variation. If d_i is twisted by the inner automorphism corresponding to d_{i+1} at the position $i = dt^*$, the product of the d components remains the identity element. It may be checked that the braid group relations are satisfied and this formula indeed defines a group action of LB_n^{BIO} on X_t .

4. Conclusions

The spin-orbit coupling is an important quantity, which is measurable in the carbon nanostructures, including the graphitic wormhole (or its nanotubular part); it can also help to identify the wormhole structure in details. SOC in a graphene could be induced by the nonzero curvature; in the particular case of the wormhole with negative curvature, the chiral fermions penetrating through the connecting nanotube in the wormhole structure could be created. The two-component Dirac equation is changed into the usual four-component form. As a consequence, the chiral fermions should be detected close to the wormhole bridge; the effect is stronger if the radius of the wormhole bridge is smaller. Moreover, one can detect permanently oriented flow when the chiral fermions prefer only one direction of the massive or massless fermionic current from the upper graphene sheet to the lower one, depending on the wormhole curvature.

We also describe the role of spinor fields in the time series of genetic code. The reversed transcription process of the gene expression could be defined by a moduli state space model of a coupling spinor field between the gene of a viral particle and the host cell. As a general result, all states of codon can be computed by the Chern-Simons 3-forms. The Chern-Simons current, coming from ghost and anti-ghost fields of supersymmetry theory, can be used to define a spectrum of gene expression in new time series data where a spinor field, as alternative representation of a gene, is adopted instead of using the alphabet sequence of standard bases A , T , C , U , and G . Effort is also directed toward the explanation of the adaptive behavior of immunosystem and to find the source of cancer from the physiology of telomere malfunction in DNA repairing state. Similar examination of Holo-Hilbert spectral analysis of the Chern-Simons current in V3 loop genotypes was performed recently in [33]. A genetic variation in V3 loop genotypes was forecast by using the imaging generated from tensor correlation network with an autoregressive integrated moving average model, support spinor model, and convolutional neural network algorithms.

The reported results of the work have promissory perspective for their extension to interdisciplinary areas as machine learning, econophysics, or biological sciences.

Acknowledgements

The work is partly supported by Scientific Grant Agency VEGA Grant No. 2/0009/19 and No. 2/0153/17. R. Pinčák would like to thank the TH division in CERN for hospitality.

IntechOpen

Author details

Richard Pinčák^{1,2} and Erik Bartoš^{3*}

1 Institute of Experimental Physics, Slovak Academy of Sciences, Košice, Slovak Republic

2 Bogoliubov Laboratory of Theoretical Physics, Joint Institute for Nuclear Research, Moscow Region, Russia

3 Institute of Physics, Slovak Academy of Sciences, Bratislava, Slovak Republic

*Address all correspondence to: erik.bartos@savba.sk

IntechOpen

© 2020 The Author(s). Licensee IntechOpen. This chapter is distributed under the terms of the Creative Commons Attribution License (<http://creativecommons.org/licenses/by/3.0>), which permits unrestricted use, distribution, and reproduction in any medium, provided the original work is properly cited. 

References

- [1] González J, Herrero J. Graphene wormholes: A condensed matter illustration of dirac fermions in curved space. *Nuclear Physics B*. 2010;**825**(3): 426-443
- [2] Pudlak M, Pincak R. Edge states of graphene bilayer strip. *European Physical Journal B*. 2013;**86**(3):1-4. Article number: 107
- [3] Castro EV, López-Sancho MP, Vozmediano MAH. New type of vacancy-induced localized states in multilayer graphene. *Physical Review Letters*. 2010;**104**(3):1-4. Article number: 036802
- [4] Castro EV, López-Sancho MP, Vozmediano MAH. Vacancy induced zero energy modes in graphene stacks: The case of abc trilayer. *Solid State Communications*. 2012;**152**(15): 1483-1488
- [5] Kochetov EA, Osipov VA, Pincak R. Electronic properties of disclinated flexible membrane beyond the inextensional limit: Application to graphene. *Journal of Physics: Condensed Matter*. 2010;**22**(39):1-11. Article number: 395502
- [6] Rostami H, Asgari R. Electronic ground-state properties of strained graphene. *Physical Review B: Condensed Matter and Materials Physics*. 2012;**86**(15):1-7. Article number: 155435
- [7] Jiang C-W, Zhou X, Xie R-H, Li F-L. Semiclassical molecular dynamics simulations for ultrafast processes in molecules. *Quantum Matter*. 2013;**2**(6): 353-363
- [8] Pincak R, Smotlacha J. Analogies in electronic properties of graphene wormhole and perturbed nanocylinder. *European Physical Journal B*. 2013;**86**(11):1-7. Article number: 480
- [9] Alhaidari AD, Jellal A, Choubabi EB, Bahlouli H. Dynamical mass generation via space compactification. *Quantum Matter*. 2013;**2**(2):140-143
- [10] Tan PH, Han WP, Zhao WJ, Wu ZH, Chang K, Wang H. The shear mode of multilayer graphene. *Nature Materials*, 11(4):294-300, 2012
- [11] Alden JS, Tsen AW, Huang PY, Hovden R, Brown L, Park J, et al. Strain solitons and topological defects in bilayer graphene. *Proceedings of the National Academy of Sciences*. 2013; **110**(28):11256-11260
- [12] Kane CL, Mele EJ. Quantum spin hall effect in graphene. *Physical Review Letters*. 2005;**95**(22):1-4. Article number: 226801
- [13] Ando T. Spin-orbit interaction in carbon nanotubes. *Journal of the Physical Society of Japan*. 2000;**69**(6): 1757-1763
- [14] Atanasov V, Saxena A. Tuning the electronic properties of corrugated graphene: Confinement, curvature, and band-gap opening. *Physical Review B: Condensed Matter and Materials Physics*. 2010;**81**(20):1-8. Article number: 205409
- [15] Pincak R, Pudlak M, Smotlacha J. *Electronic Properties of Single and Double Wall Carbon Nanotubes*. New York: Nova Science Publishers, Inc; 2012
- [16] Iorio A, Lambiase G. The hawking-unruh phenomenon on graphene. *Physics Letters, Section B: Nuclear, Elementary Particle and High-Energy Physics*. 2012;**716**(2):334-337
- [17] José MV, Zamudio GS, Morgado ER. A unified model of the standard genetic code. *Royal Society Open Science*. 2017; **4**(3):1-13. Article number: 160908

- [18] Hoffman M. Straightening out the protein folding puzzle. *Science*. 1991; **253**(5026):1357-1358
- [19] Jagadeesh A, Salam AAA, Zadeh VR, Arunkumar G. Genetic analysis of neuraminidase gene of influenza a (h1n1)pdm09 virus circulating in Southwest India from 2009 to 2012. *Journal of Medical Virology*. 2017;**89**(2): 202-212
- [20] Beyl LM. Super-lagrangians. *Physical Review D*. 1979;**19**(6): 1732-1745
- [21] Sepehri A, Pincak R. G-theory and its reduction to f (R)-gravity in FRW universe. *International Journal of Geometric Methods in Modern Physics*. 2018;**15**(9):1-15. Article number: 1850144
- [22] Capozziello S, Saridakis EN, Bamba K, Sepehri A, Rahaman F, Ali AF, et al. Cosmic space and pauli exclusion principle in a system of m 0-branes. *International Journal of Geometric Methods in Modern Physics*. 2017;**14**(6):1-32. Article number: 1750095
- [23] Antoneli F, Forger M, Gaviria PA, Hornos JEM. On amino acid and codon assignment in algebraic models for the genetic code. *International Journal of Modern Physics B*. 2010;**24**(4):435-463
- [24] Kanjamapornkul K, Pinčák R. Kolmogorov space in time series data. *Mathematical Methods in the Applied Sciences*. 2016;**39**(15):4463-4483
- [25] Capozziello S, Pincak R, Kanjamapornkul K. Anomaly on superspace of time series data. *Zeitschrift fur Naturforschung: Section A Journal of Physical Sciences*. 2017; **72**(12):1077-1091
- [26] Bartoš E, Pinčák R. Identification of market trends with string and D2-brane maps. *Physica*. 2017;**A479**:57-70
- [27] Pinčák R. The string prediction models as invariants of time series in the forex market. *Physica*. 2013;**A392**: 6414-6426
- [28] Pinčák R, Bartoš E. With string model to time series forecasting. *Physica*. 2015;**A436**:135-146
- [29] Kanjamapornkul K, Pinčák R, Bartoš E. The study of Thai stock market across the 2008 financial crisis. *Physica*. 2016;**A462**:117-133
- [30] Capozziello S, Pincak R, Kanjamapornkul K, Saridakis EN. The chern-simons current in systems of dna-rna transcriptions. *Annalen der Physik*. 2018;**530**(4):1-35. Article number: 1700271
- [31] Harley CB, Fitcher AB, Greider CW. Telomeres shorten during ageing of human fibroblasts. *Nature*. 1990;**345**(6274):458-460
- [32] Bilson-Thompson S. Braided topology and the emergence of matter. *Journal of Physics: Conference Series*. 2012;**360**:1-4. Article number: 012056
- [33] Pinčák R, Kanjamapornkul K, Bartoš E. Forecasting laurent polynomial in the chern-simons current of v3 loop time series. *Annals of Physics*. 2019;**531**:1-23. Article number: 1800375